The para-aortic ridge plays a key role in the formation of the renal, adrenal and gonadal vascular systems

磯貝純夫ら（解剖学）

ヒトの腎・副腎・性腺・尿管へ分布する動脈は、起始する位置・太さ・本数・各器官へ走行する解剖学的位置関係が変異に富んでおり、解剖学書の標準的記載は実際の1/3にしかあてはまらない。高い変異性を発生学的に説明するために、かつて激しい論争が巻き起こり、Felixの唱えるハシゴ説（ヒトの腎臓の発生過程で過渡的に出現する中腎への動脈がハシゴ状に多数残存し、ヒト成体の腎である後腎原基がこのハシゴを登ってゆく。登りきる段が異なるため変異が生ずる。）が勝利を収め、現在の発生学の教科書もこれを受け入れている。

ハシゴ説はFelix自身が述べているように推測でありながら上記血管系の変異を説明するのに便利であったため100年以上にわたって詳細に検討されることなく信じられて来た。我々は、ラット胚の血管系へ色素と樹脂を注入し、腎・副腎・性腺・尿管の動・静脈系の形成過程を追った。

Materials and methods

Rats

The vascular system develops very quickly during the early stages of development and the vascular anatomy changes rapidly until embryonic day (E)13. Therefore, we collected embryos that had been staged precisely for every 0.1-day interval fromE10.0 to E15.0. Beyond E13.0, vascular development progresses more slowly in rats and therefore we collected embryos for every 1-day interval between E15.0 and E20.0 (Table 1).

Table 1 The number of embryos injected with dye or resin at each developmental stage.

E day	Numb. Dye	Numb. Resin	E day	Numb. Dye	Numb. Resin	E day	Numb. Dye	Numb. Resin	E day	Numb. Dye	Numb. Resin	E day	Numb. Dye	Numb. Resin	E day	Numb. Dye	Numb. Resin
10.0	17	0	11.0	27	14	12.0	28	15	13.0	11	8	14.0	15	10	15.0	38	21
10.1	10	0	11.1	21	2	12.1	16	0	13.1	0	0	14.1	6	0	16.0	23	21
10.2	27	0	11.2	31	16	12.2	4	5	13.2	17	17	14.2	10	10	17.0	29	16
10.3	13	0	11.3	8	0	12.3	15	0	13.3	14	7	14.3	7	0	18.0	32	12
10.4	0	0	11.4	5	8	12.4	20	5	13.4	4	3	14.4	6	0	19.0	37	14
10.5	29	0	11.5	20	0	12.5	0	4	13.5	18	10	14.5	6	12	20.0	15	11
10.6	17	12	11.6	16	3	12.6	11	5	13.6	8	0	14.6	6	0			
10.7	16	0	11.7	15	2	12.7	25	8	13.7	6	0	14.7	6	0			
10.8	7	0	11.8	13	0	12.8	4	4	13.8	6	0	14.8	6	0			
10.9	10	6	11.9	6	9	12.9	2	5	13.9	6	0	14.9	6	0			

E day, embryonic day; Numb. Dye, number of dye-injected embryos; Numb. Resin, number of resin-injected embryos

Injection of dye

Our preliminary research suggested that the basic anatomical pattern of the renal vascular system is completed within 1 day (E14–E15). To reveal this process in detail, we applied the microdye injection technique (Ura, 1943) to embryos and prepared specimens at every 0.1-day interval during E10–E15 and at every 1-day interval during E15–E20 (Table 1).

Injection of resin

We adopted the micro-resin casting technique (Isogai & Horiguchi, 1999) to visualize the 3D morphogenesis of the fine vascular architecture within the metanephric primordium. Embryos were prepared for every 0.5- and 1-day interval during E14–E15 and E15–E20, respectively, as described above for the dye injection procedure. The umbilical vein was incised under a stereomicroscope to enable perfusion with Locke's solution initially to remove the blood and then with 2% glutaraldehyde to fix the specimen. The perfused specimens were stored temporarily in 1% paraformaldehyde that was diluted with 0.1 M PBS (pH 7.3, 4 ºC) for several days. For the injection of resin, we used embryos that were prepared within 30 min from the start of extraction of a liver because, after this period, tiny clots of blood form in the fine capillaries that prevent the perfusion of these vessels. A mixture of 30% (v / v) methyl, 17.5% (v / v) ethyl and 52.5% (v / v) 2-hydroxypropyl methacrylate monomer (Nisshin EM) was mixed with 1.5% (w / v) benzoyl peroxide 75% (Katayama Chemical) and 1.5% (v / v) N, N-dimethylaniline (Nacalai Tesque) immediately prior to the resin injection. The resin medium was then infused via a glass needle that cannulated the umbilical artery until it hardened in a plastic syringe. The injected embryos were macerated in 20% KOH solution at 40 ºC overnight and rinsed gently with DW. To remove tissues that remained adherent to the casts, we used a handmade fine water jet stream generator or an ultrasonic generator (Iuchi VS-300II). The casts were trimmed to expose the renal vascular system and frozen in water before being freeze-dried (Eiko ID-2). The casts were prepared for observation by a scanning electron microscope (SEM) as described below.

Scanning electron microscope observations

Several non-injected embryos at each developmental stage were fixed prior to SEM observation. The embryos were rinsed with 0.1 M phosphate buffer, pre-fixed with 2.5% glutaraldehyde / 0.1 M PBS for 2 h at 4 ºC, rinsed with 0.1 M PBS and post-fixed with 1% OsO_4 in PBS for 2 h at 4 ºC. They were dehydrated with 50, 70, 80, 90, and 100% ethanol, and then in 100% butanol (20 ºC) for freeze drying (Eiko ID-2). All dried specimens were mounted on metal stubs and coated with osmium (Filgen OPC 60A) before observation with an SEM (Hitachi S-4700) using an acceleration voltage of 8–10 kV.

Histology

Cryostat sections (20 lm thick) were incubated with mouse anti-rat CD31 (PECAM-1, BD Biosciences 550300), which had been diluted (÷50) in PBS-ST (0.1%, as the primary antibody for 2 h at room temperature, rinsed with PBS several times, incubated with secondary antibody, Alexa Fluor 594 goat anti-mouse IgG), which had been diluted (÷200) with PBS-ST (0.1%, for 60 min and rinsed again with PBS several times.

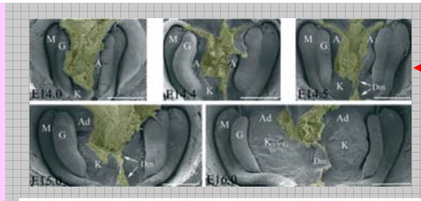

Fig. 1 Scanning electron microscope images of the urogenital / para-aortic ridge and metanephros in embryonic day (E)14.0, E14.4, E14.5, E15.0 and E16.0 rat embryos. All images are viewed from the ventral side, cranial to the top and caudal to the bottom. Nude area (not covered with peritoneum) is coloured in yellow. A, para-aortic ridge; Ad, adrenal gland; Dm, dorsal mesentery; G, genital ridge; K, metanephros; M, mesonephric ridge. White scale bar represents 500 μm in each panel.

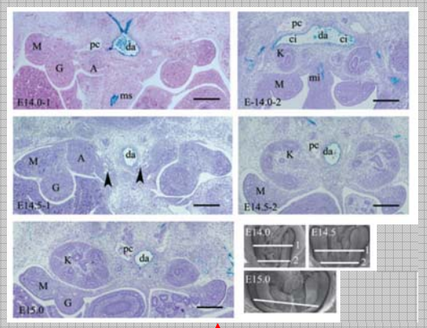

Fig. 2 Haematoxylin and eosin sections of the urogenital / para-aortic ridge and metanephros in embryonic day (E)14.0-1, E14.0-2, E14.5-1, E14.5-2 and E15.0 embryos. The arrowhead in E14.5-1 identifies the venous rete within the gonadal rete blastema. All sections are viewed from the cranial side with the dorsum to the top of the image. The white bars in the scanning electron microscope images represent the transverse cutting levels. A, para-aortic ridge; ci, common iliac artery; da, dorsal aorta (abdominal aorta); G, genital ridge; K, metanephros; M, mesonephric ridge; mi, inferior mesenteric artery; ms, superior mesenteric artery; pc, posterior cardinal vein. Black scale bar: 100 μm.

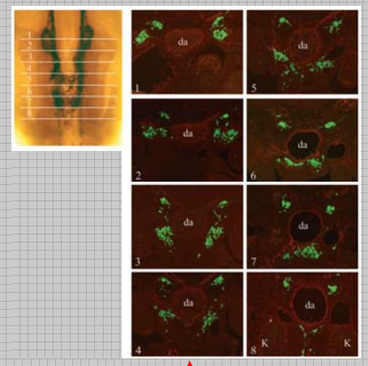

Fig. 3 Nerves and adrenomedullary cells derived from the neural crest detected by tyrosine hydroxylase reactivity (green fluorescence) around the abdominal aorta (red fluorescence) in an embryonic day 14.0 rat embryo with the dorsum of the embryo towards the top of the image in all sections. The sequence of numerals in the ventral view indicates the transverse cutting levels along the craniocaudal axis. All sections are viewed from the caudal side. da, dorsal aorta (abdominal aorta); K, metanephros.

Results

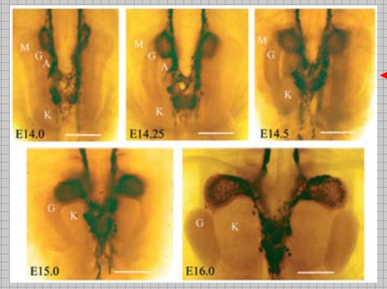

Fig. 4 Adrenal medulla, splanchnic ganglia, sympathetic trunk and nerve, and hypogastric plexus demonstrated by the presence of tyrosine hydroxylase in embryonic day (E)14.0, E14.25, E14.5, E15.0 and E16.0 embryos. The images are viewed from the ventral side with the craniocaudal axis running from the top to bottom of the images. To show the relative position of the urogenital / para-aortic ridges and the metanephros, the colour background has been adjusted. A, para-aortic ridge; G, genital ridge; K, metanephros; M, mesonephric ridge. White scale bar: 500 μm.

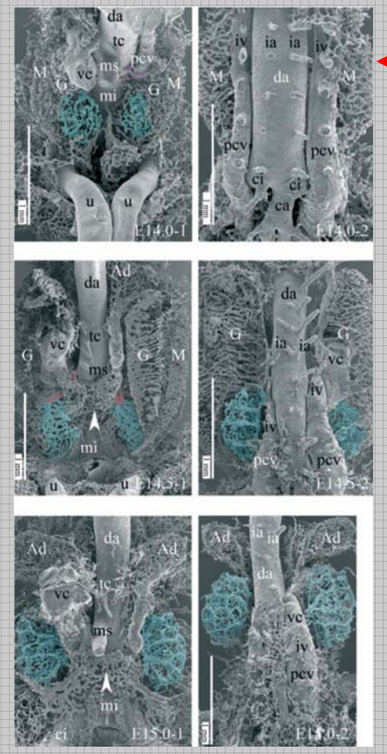

Fig. 5 Vascular resin casts of embryonic day (E)14.0 (-1, ventral view ; -2, dorsal view), E14.5 (-1 and -2) and E15.0 (-1 and -2) embryos. E14.0-1 is viewed from the cranioventral aspect to show the metanephros in the pelvis. The arterial branch to the adrenocortical anlage (E14.0-1 and 14.5-1) is coloured in pink, the gonadal rete blastema (14.0-1) and renal arteries (14.5-1) are coloured in red, and the metanephric vascular cage is coloured in blue. The white arrowhead (14.5-1 and 15.0-1) indicates the venous rete within the gonadal rete blastema. All images show the cranial aspect towards the top. Ad, adrenal gland; ca, caudal (median sacral) artery; ci, common iliac artery; da, dorsal aorta (abdominal aorta); G, gonadal sinusoid plexus; ia, intersegmental (lumbar) artery; iv, intersegmental (lumbar) vein; M, mesonephric sinusoid plexus; mi, inferior mesenteric artery; ms, superior mesenteric artery; pcv, posterior cardinal vein; tc, coeliac trunk; u, umbilical artery; vc, inferior (caudal) vena cava. White scale bar: 1 mm.

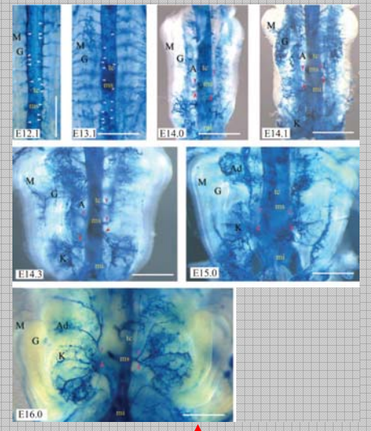

Fig. 6 Arterial branches from the abdominal aorta to the urogenital / para-aortic ridge and metanephros in embryonic day (E)12.1, E13.1, 14.0, 14.1, E14.3, E15.0 and E16.0 rat embryos visualized by injection of dye (ventral views). The white arrowheads show the remnant mesonephric arteries in the urogenital ridges, the pink arrowheads show the arterial branches to the adrenocortical anlage (E14.0, E14.1 and E14.3 embryos) or adrenal arteries (E15.0 and E16.0 embryos) and the red arrowheads demonstrate the arterial branches to the gonadal rete blastema (E14.0 and E14.1 embryos) or renal arteries (E14.3, E15.0 and E16.0 embryos). A, para-aortic ridge; Ad, adrenal gland; G, genital ridge; K, metanephros; M, mesonephric ridge; mi, inferior mesenteric artery; ms, superior mesenteric artery; tc, coeliac trunk. White scale bar: 500 μm.

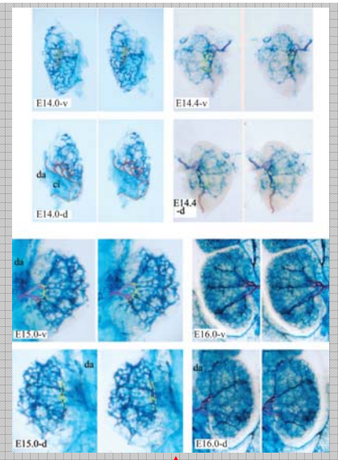

Fig. 7 Stereo view of vascular architecture within right metanephric rudiments of embryonic day (E)14.0 (-v, ventral view; -d, dorsal view), E14.4 (-v and -d) and E16.0 (-v and -d) embryos and left metanephric rudiments of an E15.0 (-v and -d) embryo visualized by injection of dye. The primary renal artery that stems from the common iliac artery is traced in red, the definitive renal artery and its anterior division are traced in pink, and the posterior division is traced in light pink. The O-shaped vascular ring around the renal hilum is traced in yellow. ci, common iliac artery; da,dorsal aorta.

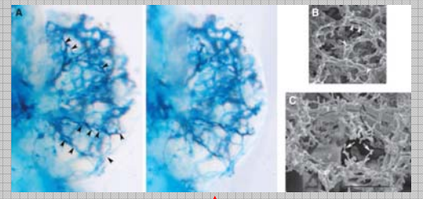

Fig. 8 (A) Fenestrations (black arrowhead) in interlobar vessels at embryonic day (E)15.0 visualized by injection of dye (stereo view). (B) Fenestrations (white arrowhead) in the arcuate vessel at E15.0, as demonstrated by a resin cast. (C) Double polygonal vascular rings that consist of an arcuate artery (A) and vein (V) at E19.0, as demonstrated by a resin cast. White arrow: interlobular artery. Black scale bar: 250 μm.

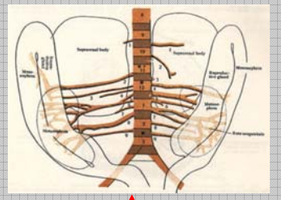

Fig. 11 A reconstruction of the mesonephric arteries of an 18-mm human embryo superimposed onto a contour drawing of a 19.4-mm embryo, after the style of Felix.

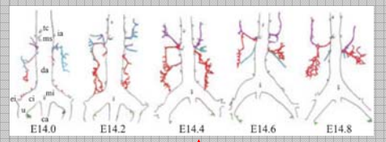

Fig. 9 Arterial branches from the abdominal aorta and iliac artery to the urogenital / para-aortic ridge and the metanephros in embryonic day (E)14.0, E14.2, E14.4, E14.6 and E14.8 rat embryos. Each arterial contour is traced from the dye-injected specimen and photographed from the ventral side. The adrenal arteries are shown in pink, the gonadal arteries are shown in blue, the mesonephric arteries are shown in green and the primary renal (ci) and renal (da) arteries are shown in red. ca, caudal (median sacral) artery; ci, common iliac artery; da, dorsal aorta (abdominal aorta); ei, external iliac artery; ia, intersegmental (lumbar) artery; mi, inferior mesenteric artery; ms, superior mesenteric artery; tc, coeliac trunk; u, umbilical artery.

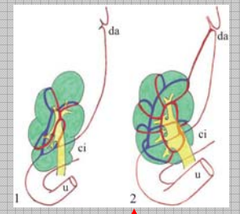

Fig. 10 Angiogenesis of primary intrametanephric circulation. The venous drainage route to the mesonephric sinusoid is not shown. (i) A primary renal artery that stems from the common iliac artery penetrates the metanephric rudiment from the dorsal (cortical) side and forms a coarse network among the mesenchymal condensations, whereas another primary renal artery forms an O-shaped vascular ring around the renal hilum. (ii) A fine vascular cage that represents the primary circulatory architecture appears within the metanephric rudiment in the pelvic region. A presumptive renal artery from the abdominal aorta reaches the vascular cage from the cranioventral side. The metanephros is shown in light green and the ureter is shown in yellow.

結語

我々の結果は、後腎が登り始める時すでに中腎動脈（ハシゴ段）が退縮していることを示し、ハシゴ説を否定した。そして、Para-aortic ridge（髄質の副腎・神経節原基と皮質の造血原基から成る）が腹側大動脈から血管芽を新たに誘導し、その発芽パターンの違いが成体の腎・副腎・性腺・尿管動脈の変異を生ずることを示した。同時に、腎静脈系と後腎原基内の動・静脈系の形態形成過程を明らかにした。

J. Anat. (2010) 216, pp656–670